PRELIMINARY ANALYSIS OF CANDIDATE ALLOYS FOR USE IN THE CANDU-SCWR

W. Cook[1], J. Miles[1], J. Li[2], S. Kuyucak[2], W. Zheng[2]

[1]University of New Brunswick, Fredericton, New Brunswick, Canada
[2]CANMET-MTL, Ottawa, Ontario, Canada

Abstract

The newly commissioned test loop at the University of New Brunswick was used to test two ferritic steels as potential candidates for use in the CANDU-SCWR. The first steel comprised of 14%-Cr was selected as the base metal for processing into an oxide dispersion strengthened (ODS) steel. Due to its good corrosion resistance but relatively low ductility, the second steel with 25%-Cr has been considered as a coating material. Coupons cut from both alloys were exposed to supercritical water in the as-cast, as-rolled, and rolled plus homogenized conditions. Corrosion experiments took place at 500°C and 25 MPa for durations of 100, 250 and 500 hours. The purpose of this study was to examine the corrosion rate and oxide formation characteristics for these two steels. Preliminary weight change results indicate weight gain increasing with exposure time for the 14%-Cr steel. This correlates with the growth of a continuous dual layer oxide as seen in cross-sectional SEM work. The inner layer consists of a chromium-rich, iron-depleted oxide, while the outer layer is an iron-rich oxide deposited on the surface. For the 25%-Cr coupons, the weight change was very small, in agreement with the SEM work that showed very little oxide growth.

Keywords: Materials, Corrosion, ODS, CANDU-SCWR

1. Introduction

The Generation IV International Forum (Gen IV) is a global initiative established to develop the next generation of nuclear reactors. This organization plans and coordinates collaborations between GEN IV research programs in several countries around the world, to develop these future nuclear power systems and components. Of the six concepts being considered for the next generation design, two of the most promising options are the SCWR (Supercritical Water-cooled Reactor) and the VHTR (Very High Temperature Reactor). These two reactor concepts differ in the cooling fluid used along with the operating conditions within the heat transport system [1].

In Canada, the SCWR is being developed as the natural progression from the current CANDU design. Researchers at academic institutions and in government laboratories (including Atomic Energy of Canada Limited (AECL), the Material Technology Laboratory (MTL) of NRCan and the National Research Council (NRC)) are working together to advance the knowledge base required to develop various in-core and out-core components. In particular, materials for the fuel cladding and coolant piping are being assessed, and in some cases developed, for operation under these extreme conditions. Material improvements include new alloys and surface coatings with increased resistance to high temperature creep, general corrosion and stress corrosion cracking (SCC). The work outlined here details the operation of a supercritical water test loop to

determine the resistance to corrosion and SCC of the candidate materials in an environment simulating some of the proposed reactor operating conditions. In the CANDU-SCWR concept, the light coolant water enters the reactor core as sub-critical water, and at the outlet, the water will be in the supercritical state with a temperature of 625 °C at 25 MPa. Thus, the coolant experiences a range of temperatures and densities as it passes through the core. For the work reported in this paper, the test condition was set at 25 MPa and 500°C.

Samples of new alloys and surface coatings are provided through a partnership with CANMET-Materials Technology Laboratory, NRCan (Natural Resources Canada), AECL (Atomic Energy of Canada Limited) and the NRC (National Research Council). The purpose of this study is to develop the most effective alloys and surface coating configurations for use in the SCWR system. Collaboration between government, academia and industry provides the necessary mechanism to assess and improve upon existing and novel alloys [2].

2. Experimental

In order to study the corrosion of candidate alloys under conditions simulating those of the CANDU-SCWR, a dynamic test loop has been constructed in the nuclear laboratories in the Department of Chemical Engineering at UNB. A piping and instrumentation diagram of the system is shown in Figure 1. This continuous flow system has a capacity for a flow rate of 500 ml/min and can operate under a wide range of conditions above the critical point. Deionized water from a reservoir is pressurized with a positive displacement pump to a pressure of 25 MPa. This water is initially heated with water returning from the system using a tube-in-tube interchanger with high temperature process fluid. The water is then heated through the critical point to the operating temperature of interest, in the case of this study, 500°C. It then passes through a pressure vessel (autoclave) in which the test coupons are suspended for exposure. Hot fluid then passes back through the tube-in-tube interchanger where it is cooled through the critical point. Before returning to the reservoir, the returning process fluid is brought to ambient conditions through a chilled water cooler and pressure regulating valve.

Control systems are in place to monitor and regulate conditions within the system. Flow rate, temperature, pressure and conductivity are all recorded and logged to a database using data acquisition software. Safety measures are programmed into the loop control software making this an inherently safe system. Under low flow, high pressure and high temperature conditions, the loop will shut down automatically, reducing the effect of these incidents.

Polished test coupons are suspended on a tree placed inside the autoclave, Figure 2. These coupons are placed in duplicate within the autoclave to allow for both SEM and weight change analyses.

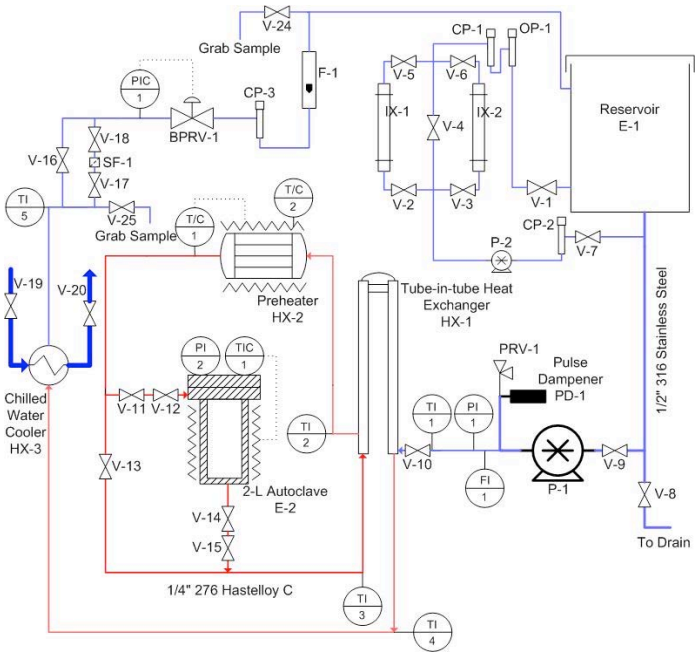

Figure 1. Schematic of UNB's supercritical water test loop.

Figure 2. Picture of coupon tree loaded with samples of the two steels.

Two ferritic steels were cast at CANMET-MTL and tested under supercritical water conditions. The first material was a 14% Cr steel based on the MA957 oxide-dispersion strengthened (ODS) alloy, designated by its Heat No. V9011. This alloy was chosen as the base steel for oxide dispersion strengthening to achieve high creep strength and radiation resistance [3]. Above 14% chromium, ferritic steels become susceptible to embrittlement by the precipitation of ordered phases (sigma, chi, etc.) when held at the service temperatures considered for the SWCR fuel

cladding (600-850°C). Therefore, for corrosion protection, a second steel containing 25% Cr, designated as V9012 in MTL's internal tracking system, was selected to be used as a coating alloy to provide further corrosion resistance of the ODS structural alloy. Ferritic based alloys are known to have superior heat transfer properties and their SCC resistance in SCW is much greater than the common austenitic or Ni-based alloys.

Casting began with 220 kg vacuum melts and yielded four 50 kg ingots in cast-iron book molds. The ingot dimensions were 5×6×12", and they were labeled by their Heat No. and their casting sequence. Three 3/8" thick bottom plates were taken from the "A" ingots (A1 to A3). As-cast samples were taken from the ingot edge, and therefore contained the chill zone.

After removing the risers and bottom plates, 5×6×3" billets were cut from the A-ingots. These were reheated to 1200°C for 2.5 hours and hot rolled from 3" to 3/8" thick plates with a cross-roll after the first pass. The plates were fan-cooled after the finishing pass to prevent the formation of the embrittling (sigma, chi) phases. Two-thirds of the hot-rolled plates were homogenized at 1200 °C for 8 hours. The plates were furnace cooled to 850 °C and were subsequently removed and fan cooled one by one to avoid the precipitation of embrittling phases.

Coupons were cut from these steel plates obtained from CANMET-MTL in Ottawa. Approximate dimensions for these coupons were 20x10x2 mm and a 2 mm hole was drilled near one edge for mounting. Each coupon was labeled using a unique identifier and all coupons were polished to an 800 grit finish. The dimensions of the coupons were measured using a set of callipers with a precision of ±0.01 mm. The coupons were then weighed using an analytical balance with a precision of ±0.1 mg. After polishing, coupons were stored in acetone and dried in air before mounting on the tree for exposure tests.

The first experimental run after loop commissioning tested the corrosion characteristics of two ferritic steels with three different surface treatments. Coupons were exposed to supercritical water at 500°C and 25 MPa for increasing durations up to 500 hours. The chemical compositions of the two steels that were cast and tested are shown in Table 1.

Table 1. Elemental compositions of the steels tested (wt. pct.).

Heat No.	Aim Cr	Cr	Mo	C	Si	Mn	Cu	P	S	O	N
V9011	14-Cr	14.4	0.30	0.022	<0.010	0.076	<0.010	0.004	<0.002	0.017	0.012
V9012	25-Cr	24.8	0.30	0.022	<0.010	0.046	<0.010	0.004	0.002	0.024	0.012

Each of these steels was tested in the as-cast, as-rolled, and rolled plus homogenized states. The six distinct coupon types were placed in duplicate within the autoclave; one set was used for weight change measurements and the other set for surface characterization. For the 500°C run, coupons were placed in the autoclave with a flow rate of approximately 200 g/min of deoxygenated supercritical water with a dissolved oxygen concentration of approximately 25 ppb or less. After 100 hours, the loop was shut down and the coupons were removed and placed in a desiccator before weighing. Two sets of coupons were placed in the autoclave and the loop was

run for a further 250 hours. At this point, one set was removed and the remaining coupons were left for an additional 250 hours of exposure.

After exposure, select coupons were characterized using scanning electron microscopy (SEM) at both the University of New Brunswick and CANMET-MTL. Plan view images were collected for one of every coupon type that was exposed. From these results, nine coupons were then prepared for cross-sectional SEM work to cover a range of test exposures and surface preparations. Each of these nine pieces was cut using a small hacksaw without cutting fluid. A light burst of nitrogen was used to clean the coupons after they were cut and they were handled delicately with vinyl gloves.

At the Material Technology Laboratory, the sectioned coupons were mounted in an epoxy resin. Each sample had approximately 1 mm removed with a coarse polisher to eliminate any mechanical damage during the cutting. The surfaces were then polished to a 1μm finish and coated with gold before examination in the SEM facility.

3. Results and Discussion

For each of the alloys and surface treatments tested, two coupons were exposed for increasing durations. Weight change measurements were used on one set to quantify the corrosion rate. SEM analysis and FIB cross-sectioning were carried out on the remaining coupons. The following trends were observed for corrosion rates at increasing time intervals (Figure 3).

As evident in Figure 3 there is a clear difference between the corrosion characteristics of the 14 Cr (V9011) and 25 Cr (V9012) samples, but little difference in the overall corrosion behaviour between the different processing finishes. As observed with the naked eye, the 14 Cr steels showed a matte appearance, which was attributed to the continuous oxide film present on the entire coupon surface. The 25 Cr steel coupons retained their metallic sheen after exposure with only small regions of localized attack. These results were supported with plan view and cross-sectional SEM work (see below). From the growth kinetics shown in Figure 3, the 14 Cr steel is seen to follow a power-law kinetic relation between the weight change and the exposure time ($\Delta w = c\, t^n$), with the value of n being about 0.9.

Most of the 25 Cr steel samples experienced a slight weight loss. This trend agrees with the qualitative results obtained from the SEM images, shown in Figure 4 (a-f) and Figure 5 (a-f). In plan view, for both the as-cast (B-2) and homogenized (B-8) coupons, the original polished surface remains largely unaffected with localized attack evident on or near grain boundaries. Further, in cross-section, it is apparent that oxidation is restricted to small nodules on the surface with minimal penetration into the substrate on the bulk of the sample. The formation of these nodules on the high chromium material is quite unusual and unexpected and a detailed study of the mechanism of their formation and growth is discussed elsewhere [4].

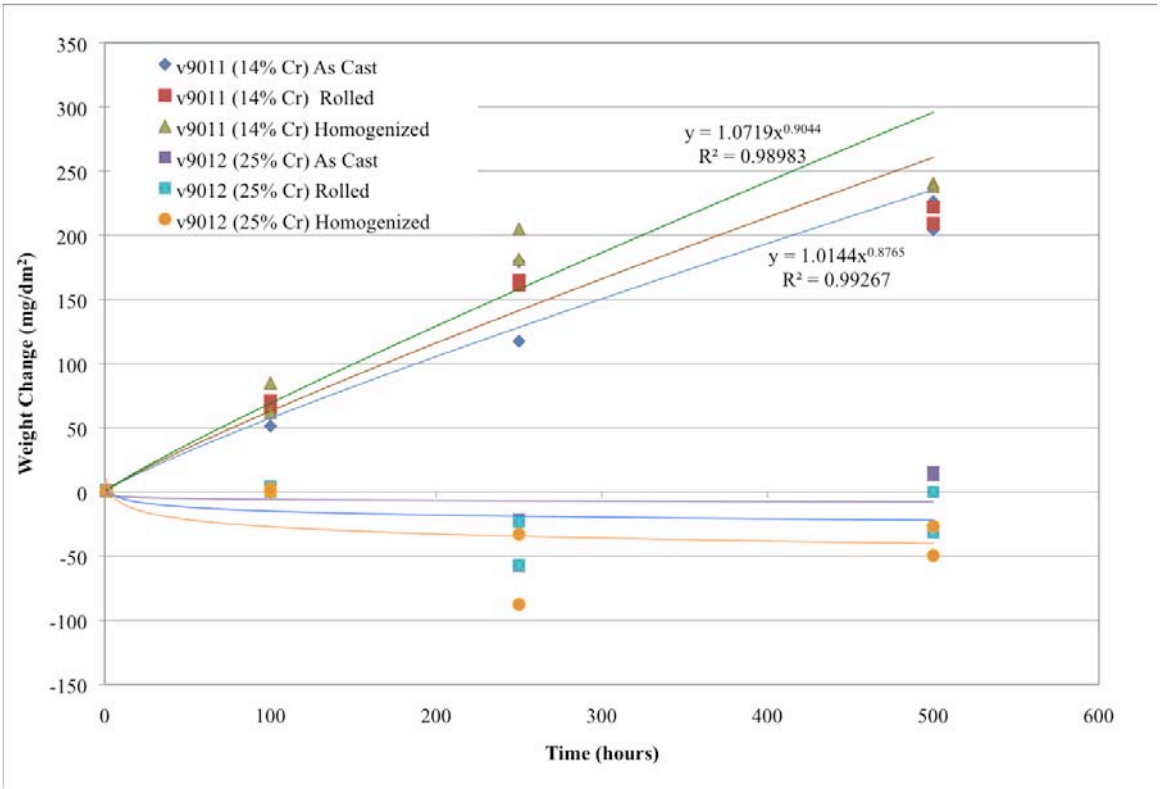

Figure 3. Weight change of the 14% Cr (V9011) and 25% Cr (V9012) samples in each state of preparation exposed in 500°C, deoxygenated supercritical water.

In this study, the corrosion products that formed on the surfaces in Figure 4 and 5 were characterized using EDS to determine the oxide distribution in the film. This analysis showed a well-defined double layer oxide. The inner layer was comprised of a chromium-rich oxide extending from the original coupon surface into the substrate; the outer layer developed above the original surface, and appeared to be iron-rich oxide. It is interesting to note that for every nodule of iron oxide on the outer surface, there is a corresponding penetration of chromium-rich oxide extending into the substrate that is a more-or-less perfect mirror image of the nodule. The iron diffusing outward into the bulk SCW creates an iron-deficient region just below the surface, effectively inducing a chromium enrichment zone immediately below the coupon surface.

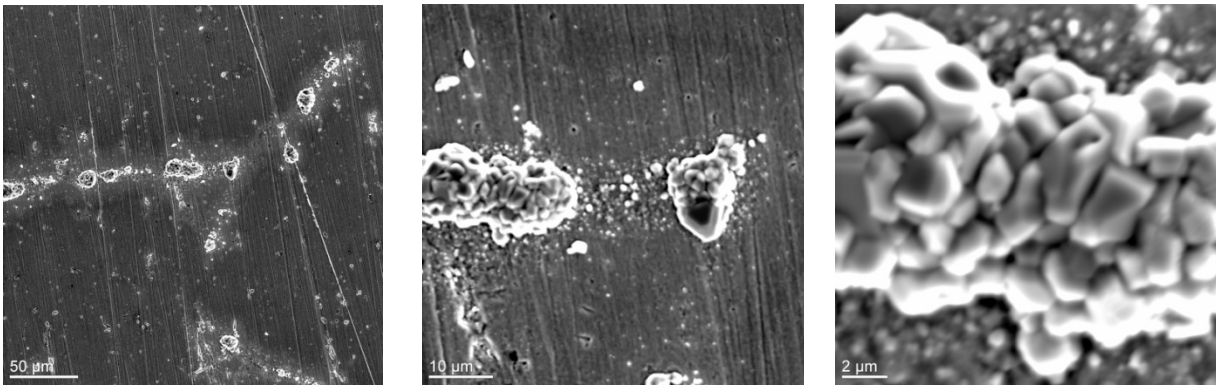

(a) B2-300x (b) B2-1400x (c) B2-5000x

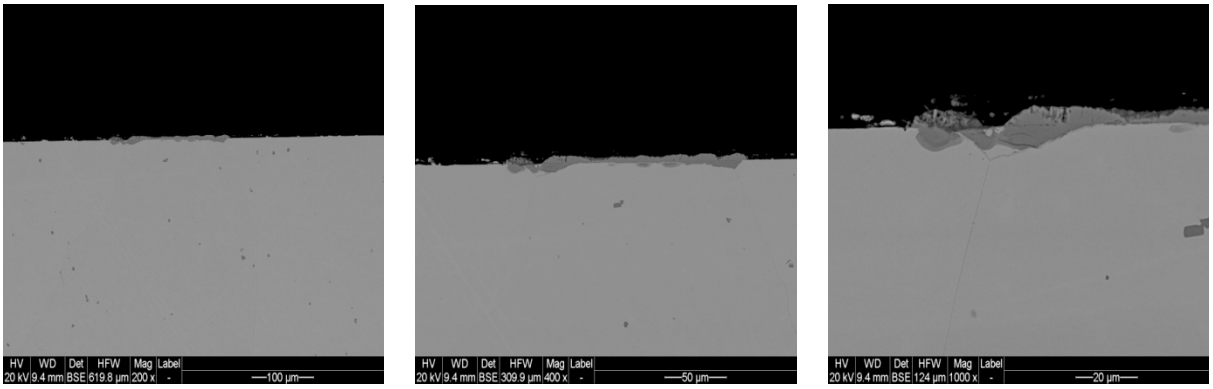

(d) B2-2-400x (e) B2-2-1000x (f) B2-2-2000x

Figure 4- Plan and cross-sectional views at increasing magnifications of the as-cast V9012 (25% Cr) coupon exposed for 500 hours in 500°C deoxygenated supercritical water.

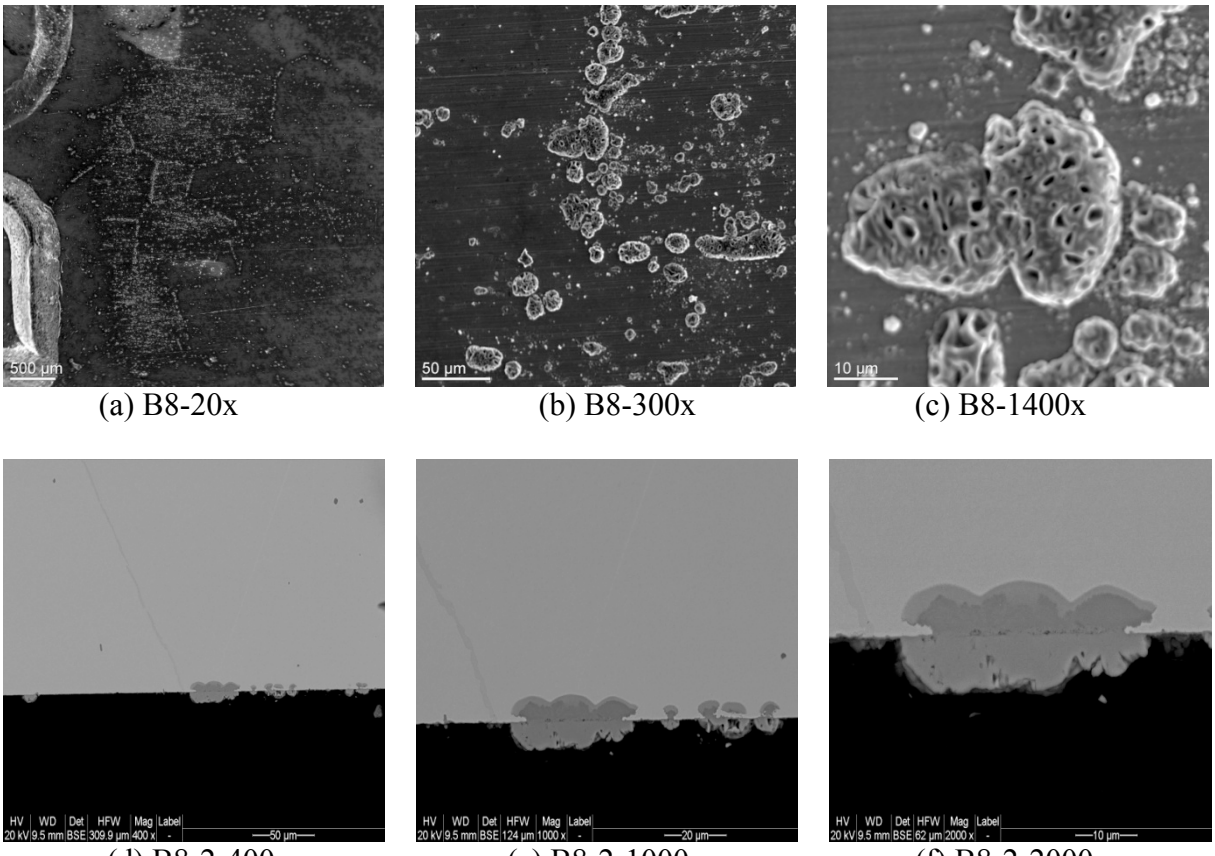

(a) B8-20x (b) B8-300x (c) B8-1400x

(d) B8-2-400x (e) B8-2-1000x (f) B8-2-2000x

Figure 5. Plan and cross-sectional views at increasing magnifications of the homogenized V9012 (25% Cr) coupon exposed for 500 hours in 500°C deoxygenated supercritical water.

Since the nodules are highly localized, usually occurring adjacent to grain boundaries, it is likely that they result from local effects, possibly the precipitation of undesired phases near the grain boundaries. The 25 Cr steel was supplied in the homogenized condition but before the corrosion

testing began, the steel was studied for evidence of intergranular sensitization. The light microscopy image in Figure 6a shows the presence of intergranular films. EDX analysis showed the grain boundary film to be rich in chromium, which would lead to the steel's sensitization. The exact phase of the grain boundary precipitate is currently under investigation.

In contrast to the 25% Cr steel (V9012), the 14% Cr steel (V9011) trend lines in Figure 3 show considerable weight gain for each processing finish. The gain in weight due to increasing oxidation with exposure time followed a nearly linear power dependence. Qualitatively, this oxidation was observed as a continuous oxide film present at the shortest exposure and growing in thickness as exposure time increased. SEM work conducted in plan view revealed the oxide as tightly packed octahedral crystals uniformly distributed across the coupon. In cross-section, the same dual-layer oxide as with the 25% Cr coupons was observed; however, the film was continuous and none of the original substrate remained visible. EDS indicates that the oxide film is predominately iron, presumably magnetite. It is interesting to note the apparent porosity in the outer oxide film in Figure 7 a-c. It appears as if the magnetite was precipitated from solution at some locations as tubes. This tubular oxide structure was previously reported in supercritical water oxidation of ferritic steels and, in one case, was attributed to elemental impurities in the substrate [5, 6]. Regardless of the cause or mechanism of the porosity formation, it is apparent that such porosity may act as a short-circuit pathways for the release of corrosion products from the base material.

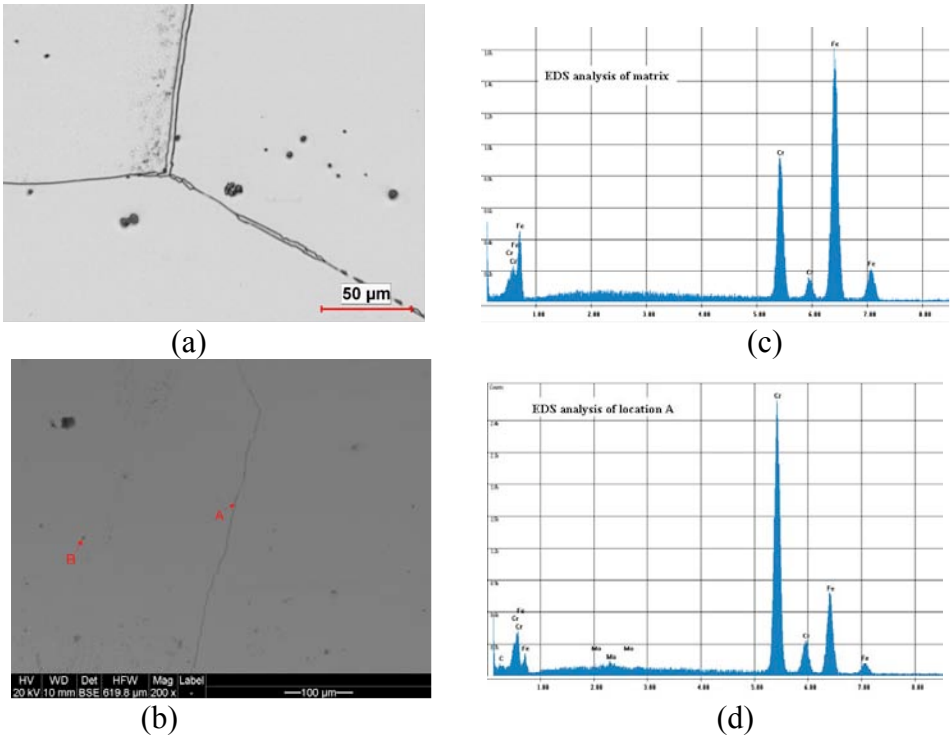

Figure 6. Etched surface of a homogenised 25 Cr steel (soaked at 1200°C for 8 h, furnace cooled to 850°C and fan cooled to room temperature. (a) light microscope image showing film-like grain boundary phases, (b) SEM image, (c) EDX of matrix and (d) grain boundary phase, showing accumulation of Cr at the grain boundary phase.

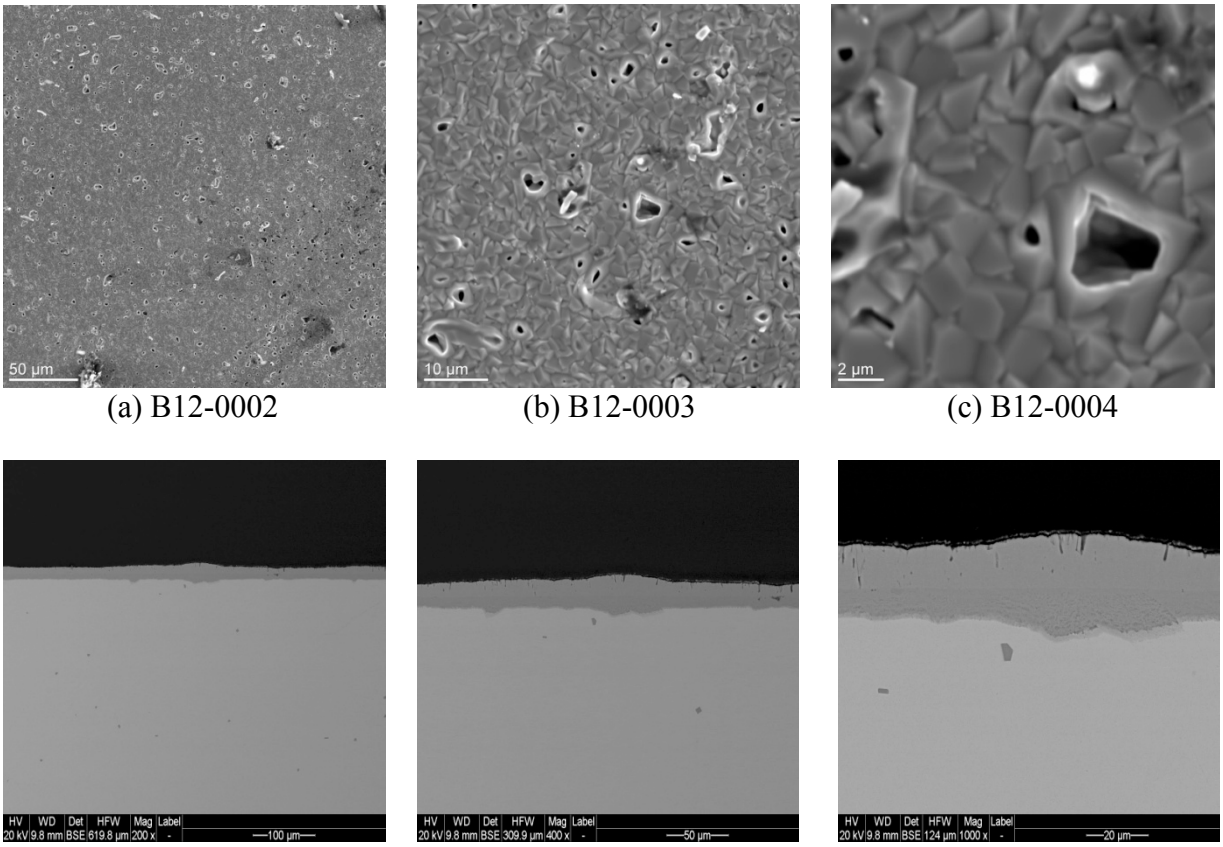

(a) B12-0002 (b) B12-0003 (c) B12-0004

(d) B12-2-002 (e) B12-2-003 (f) B12-2-004

Figure 7. 14% Cr as-cast coupon exposed for 500 hours.

The images in Figure 8 show the progression of the continuous oxide film formation on the surface of the 14 Cr steel as exposure time increased. Each of these images, taken at the same magnification, represents the same alloy exposed at (a) 100 hours (b) 250 hours and (c) 500 hours. Evaluating the oxide thickness over time shows growth as 0, 6, 15 and 18 µm at 0, 100, 250 and 500 hours respectively.

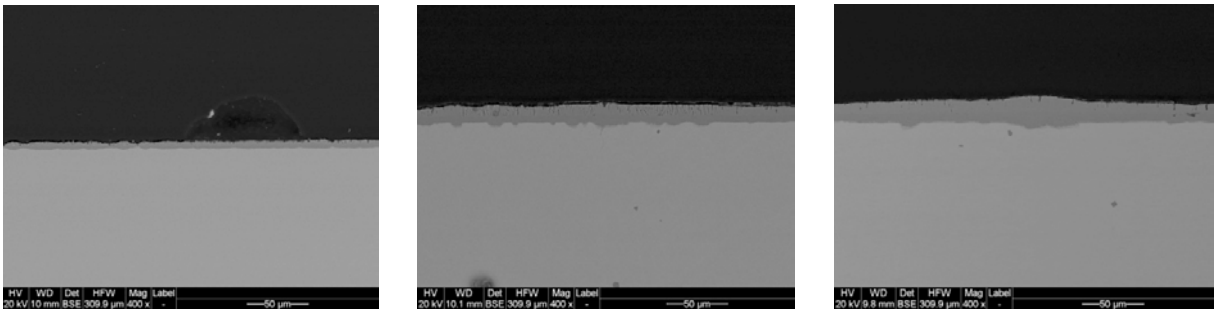

(a) 100 hours (b) 250 hours (c) 500 hours

Figure 8. Progression of oxide film formation on the 14% Cr steel.

At the longest exposure time for the 14 Cr steel, high resolution SEM pictures showed additional complexity in the two layer oxide structure. The leading edge of the Cr-rich front moving into

the substrate appears to be a transition zone with an intermediate composition between that of the substrate and the oxide.

To examine the continuous double oxide layer in detail, further analysis was done on the 14 Cr as-cast coupons above. EDS maps were collected to determine the elemental distribution in the corroded zone, Figure 9.

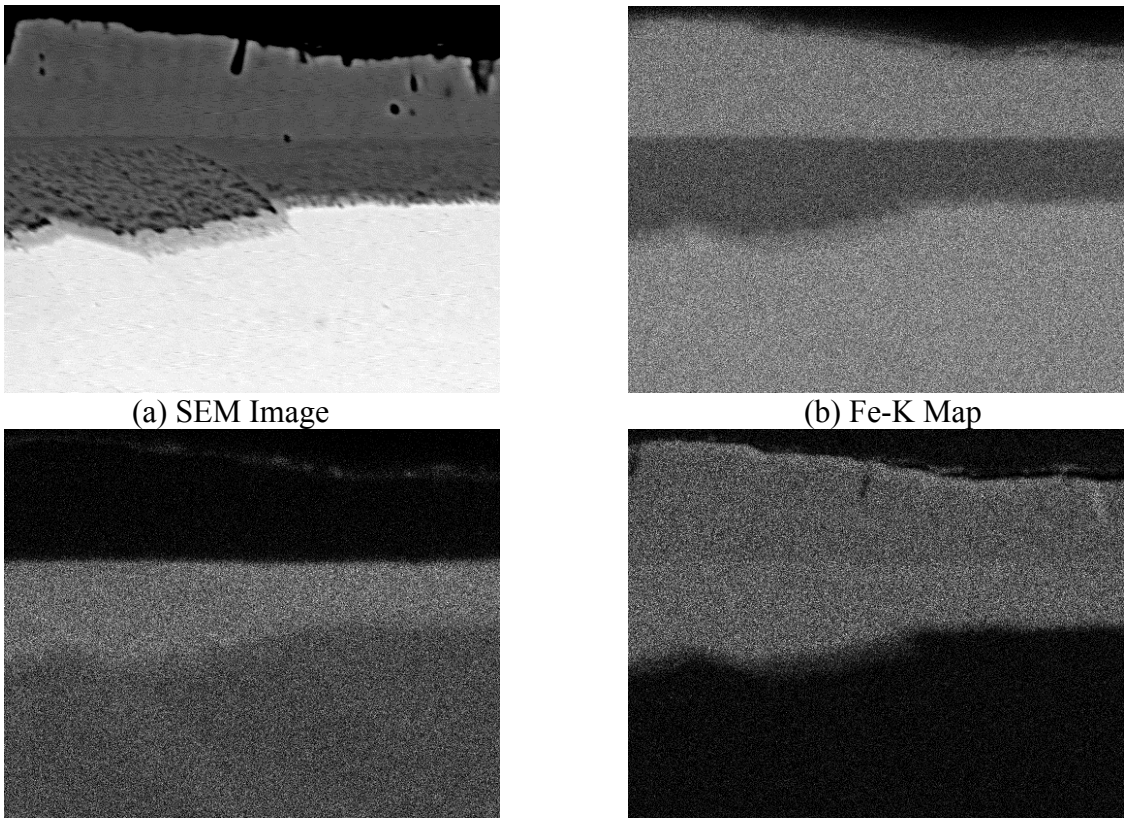

(a) SEM Image (b) Fe-K Map

(c) Cr-K Map (d) O-K Map

Figure 9. EDS Element Mapping of Dual Layer Oxide.

Element maps in Figure 9 confirm the structure of the oxides observed in cross-section for all of the coupons studied. An inner Cr-rich oxide developed as iron dissolved into the bulk supercritical water adjacent to the coupon. Additionally, an iron oxide layer deposited onto the outside of the coupon surface. In Figure 9 (a), there is a visible difference between the chromium oxide and the substrate in the transition zone. The EDS map in Figure 9 (d) indicates that this zone has elevated oxygen content. The transition zone could be a region of internal oxidation sustained by the inward diffusion of oxygen from the surface.

4. Conclusions

A dynamic test loop was established at the University of New Brunswick to study the corrosion of candidate alloys for use in the CANDU-SCWR. Preliminary supercritical water exposure tests

on two ferritic steels have been conducted and are presented. A lower chromium (14% Cr) steel was produced as it is a potential steel for ODS processing, while a higher chromium (25% Cr) steel has been considered because of its potential as a coating material. Weight change data was recorded and detailed SEM work was completed to characterize the surface oxidation. The 14% Cr samples demonstrated a significant susceptibility to general corrosion in tests up to 500 hours at a temperature of 500°C. A continuous oxide double-layer formed on the coupons that consisted of a chromium-rich layer extending into the substrate and an iron-rich outer layer formed on the surface. Even at longer exposure times, the 25% Cr samples demonstrated good oxidation resistance overall with negligible weight gain observed. However, intergranular corrosion was encountered that resulted from the sensitization caused by the precipitation of a Cr-rich phase.

5. Acknowledgements

The authors are grateful for the financial support of NSERC/NRCan/AECL Generation IV Technologies Program and the MTL RIEM program for performing this work. Dr. Douglas Hall and Steven Cogswell (UNB) along with Ms. Pei Liu and Ms. Renata Zavadil (CANMET) are thanked for their help with SEM imaging and preparation for the metallographic samples. Colin Bradley is thanked for his continuing help with performing the experiments.

6. References

[1] Duffey, R. (2004), CANDU and Generation IV Systems. *Abstracts of the Pacific Basin Nuclear Conference*, (pp. 273-277).

[2] Brady, D. et al (2009), Canada's NSERC/NRCan/AECL Generation IV Energy Technology Program, *Proceedings of the 30th Annual Conference of the Canadian Nuclear Society*, Calgary.

[3] Odette, G. R. et al. (2008), Recent Developments in Irradiation-Resistant Steels. *Annu. Rev. Mater. Res*., v.38, 471-503.

[4] Miles, J., Artymowicz, D., Newman, R., Cook, W., & Botton, G. (2010), Preliminary study of oxidaion mechanisms of high Cr steel in SCW. *Accepted to the 2nd Canada-China Joint Workshop on SCWR.*

[5] Chen, Y., Sridharan, K., & Allen, T. (2006), Corrosion behaviour of ferritic-martensitic steel T91 in supercritical water. *Corroison Science , 48* (9), 2843-2854.

[6] Tan, L., & Allen, T. (2009), Localized corroison of magnetite on ferritic-martensitic steels exposed to subercritical water. *Corrosion Science , 51*, 2503-2507.